Journal of Organometallic Chemistry 1012 (2024) 123147

Contents lists available at ScienceDirect

Journal of Organometallic Chemistry

journal homepage: www.elsevier.com/locate/jorganchem

Nitrosyl derivatives of the halide-bridged complexes $[M_2Cp_2(\mu\text{-}X)(\mu\text{-}P^tBu_2)(CO)_2]$ (M = Mo, W; X = Cl, I).

M. Angeles Alvarez, M. Esther García, Daniel García-Vivó *, Ana M. Guerra, Miguel A. Ruiz *

Departamento de Química Orgánica e Inorgánica/IUQOEM, Universidad de Oviedo, E-33071 Oviedo, Spain

ARTICLE INFO

Keywords:
Nitrosyl complexes
Carbonyl complexes
Halide complexes
Hydride complexes
Cyclopentadienyl ligands
Imide ligands

ABSTRACT

The title compounds were prepared as described previously (M = Mo, X = Cl) or by the reaction of the known unsaturated complex $[W_2Cp_2(\mu\text{-}P^tBu_2)(CO)_4]BF_4$ with NaI in refluxing 1,2-dichloroethane solution. Reaction of these halide-bridged complexes with NO (1 atm) at low temperature yielded the corresponding dinitrosyl derivatives *syn,trans*-$[M_2Cp_2X(\mu\text{-}P^tBu_2)(CO)(NO)_2]$, with a *syn* arrangement of Cp ligands relative to the M_2P plane, and a transoid arrangement of the halide ligand X relative to the P atom, according to an X-ray study on the ditungsten complex ($W{-}W$ = 3.113(1) Å). Further decarbonylation of these products at high temperature yielded in both cases the halide-bridged complexes *trans*-$[M_2Cp_2(\mu\text{-}X)(\mu\text{-}P^tBu_2)(NO)_2]$ as major products, but the minor products were different. For the molybdenum complex, an isomer of the final product, *cis*-$[Mo_2Cp_2(\mu\text{-}Cl)(\mu\text{-}P^tBu_2)(NO)_2]$, was formed. In contrast, the minor tungsten product, *anti,cis*-$[W_2Cp_2I(\mu\text{-}P^tBu_2)(CO)(NO)_2]$, was an isomer of the parent complex. In addition, trace amounts of the imide cyclopentadienylidene complex $[W_2Cp(\mu\text{-}\kappa{:}\eta^5\text{-}C_5H_4)I(\mu\text{-}P^tBu_2)(NH)(NO)]$ was also obtained ($W{-}W$ = 2.9376(2) Å). Density functional theory calculations were used to examine possible routes to the above dinitrosyl complexes, that seem to involve at least three reaction pathways: direct decarbonylation, rearrangement of the MCpX(NO) fragment prior to decarbonylation, and rearrangement of the MCp(CO)(NO) fragment prior to decarbonylation.

1. Introduction

Recently we reported the formation of the chloride-bridged dinitrosyl complex $[Mo_2Cp_2(\mu\text{-}Cl)(\mu\text{-}P^tBu_2)(NO)_2]$ (**3a**) from the corresponding dicarbonyl complex $[Mo_2Cp_2(\mu\text{-}Cl)(\mu\text{-}P^tBu_2)(CO)_2]$ (**1a**), in a two step process involving an intermediate species (presumably $[Mo_2Cp_2Cl(\mu\text{-}P^tBu_2)(CO)(NO)_2]$ (**2a**)) not characterized at the time (Scheme 1) [1]. Interest in this sort of halide-bridged species stems from their potential as precursors for unsaturated nitrosyl hydrides and anions, a scarce group of compounds which, however, can display a rich chemistry, as evidenced by the reactivity of the ditungsten complexes $[W_2Cp_2(\mu\text{-}PPh_2)(NO)_2]^-$, and $[W_2Cp_2(\mu\text{-}H)(\mu\text{-}PPh_2)(NO)_2]$. The latter are two PPh_2-bridged complexes which can be readily prepared upon reduction of the iodide-bridged complex $[W_2Cp_2(\mu\text{-}I)(\mu\text{-}PPh_2)(NO)_2]$ [2,3]. Surprisingly, however, the reduction of the P^tBu_2-bridged dimolybdenum complex **3a** with Na(Hg) in acetonitrile solution did not yield the expected unsaturated anion $[Mo_2Cp_2(\mu\text{-}P^tBu_2)(NO)_2]^-$ [1], but instead led to products derived from unusual C≡N and N≡O bond cleavages of acetonitrile [4] and nitrosyl ligands [5,6], depending on reaction conditions. It was not clear whether this big difference in chemical behaviour might be attributed to the change in metal (W vs. Mo) or in the PR_2 ligand (Ph vs. ^{t}Bu), or both. Thus, we seek to implement convenient synthetic routes for new P^tBu_2-bridged ditungsten complexes analogous to the dimolybdenum complex **3a**, which is the main target of the present work. This in turn required a revision of the synthesis of the electron-precise precursor $[W_2Cp_2(\mu\text{-}H)(\mu\text{-}P^tBu_2)(CO)_4]$ [5a], whereby a novel unsaturated hydride has been now unveiled. In addition, we have also revised our preliminary preparation of **3a**, this including the characterization of the elusive intermediate **2a**. As it will be shown below, the new experimental work indicates that the transformations connecting complexes **1** and **3** are more complex than anticipated, and that there are side reactions leading to minor, but interesting products.

* Corresponding author at: Departamento de Química Orgánica e Inorgánica/IUQOEM, Universidad de Oviedo, E-33071 Oviedo, Spain.
E-mail addresses: garciavdaniel@uniovi.es (D. García-Vivó), mara@uniovi.es (M.A. Ruiz).

https://doi.org/10.1016/j.jorganchem.2024.123147
Received 21 March 2024; Received in revised form 11 April 2024; Accepted 16 April 2024
Available online 20 April 2024

Scheme 1. Formation of the dinitrosyl dimolybdenum complex **3a**.

2. Results and discussion

2.1. Revision of the preparation of $[W_2Cp_2(\mu\text{-}H)(\mu\text{-}P^tBu_2)(CO)_4]$: Synthesis and structural characterization of the unsaturated hydride $[W_2Cp_2H(\mu\text{-}P^tBu_2)(CO)_2]$ (4)

In a preliminary work we reported the formation of the tetracarbonyl hydride complex $[W_2Cp_2(\mu\text{-}H)(\mu\text{-}P^tBu_2)(CO)_4]$ upon reaction of diglyme solutions of $[W_2Cp_2(CO)_4]$ with HP^tBu_2 at 353 K [5a]. We have now slightly improved the overall isolated yield of this complex by replacing the diglyme solvent with propylbenzene from start (preparation of $[W_2Cp_2(CO)_4]$), and by increasing to 363 K the temperature after addition of phosphine (Scheme 2). However, then we observe the formation of small amounts (ca. 3 %) of a dark green complex which we have identified as the new unsaturated hydride $[W_2Cp_2H(\mu\text{-}P^tBu_2)(CO)_2]$ (**4**) (see below). This was fully unexpected, since previous studies from our lab on decarbonylation of PPh_2- or PCy_2- bridged complexes of type $[M_2Cp_2(\mu\text{-}H)(\mu\text{-}PR_2)(CO)_4]$ (M = Mo, W) failed to yield any unsaturated hydrides of type $[M_2Cp_2H(\mu\text{-}PR_2)(CO)_2]$ [7]. The latter complexes, instead, had to be prepared through more laborious routes involving the participation of the unsaturated halide-bridged complexes $[M_2Cp_2(\mu\text{-}X)(\mu\text{-}PR_2)(CO)_2]$, and of the triply-bonded anions $[M_2Cp_2(\mu\text{-}PR_2)(\mu\text{-}CO)_2]^-$ (M = Mo, R = Ph, Cy [8]; M = W, R = Cy) [9], in a process that we could extend more recently to the Mo analogue of **4** [10]. Since these unsaturated hydrides display a rich chemistry [11], it was therefore of interest to see whether hydride **4** could be efficiently prepared by the thermal decarbonylation of $[W_2Cp_2(\mu\text{-}H)(\mu\text{-}P^tBu_2)(CO)_4]$, because this would greatly simplify the synthetic route to such an unsaturated species, thus eventually enabling a more in-depth study of its chemical behaviour in the future. Indeed we have found that refluxing toluene solutions of the above tetracarbonyl hydride complex very slowly yields the targeted dicarbonyl **4** as the unique P-containing product, although full conversion is more conveniently reached (in ca. 2.5 h) in refluxing propylbenzene solutions (ca. 433 K). In this way, compound **4** can be isolated in ca. 25 % yield after chromatographic workup (Scheme 2).

Spectroscopic data for the hydride $[W_2Cp_2(\mu\text{-}H)(\mu\text{-}P^tBu_2)(CO)_4]$ [5a] are comparable to those of related PCy_2-bridged complexes reported by us [7], or to those of the related dimolybdenum complex $[Mo_2Cp_2(\mu\text{-}H)(\mu\text{-}P^tBu_2)(CO)_4]$ [12], and deserve no specific discussion. We just note that the hydride ligand gives rise to a characteristic highly shielded ^1H NMR resonance at −16.29 ppm displaying a moderate coupling to both ^{31}P and ^{183}W nuclei (J_{HP} = 25 Hz, J_{HW} = 40 Hz; cf. δ −16.4 ppm; J_{HP} = 24; J_{HW} = 40 Hz for the related PCy_2-bridged complex) [7].

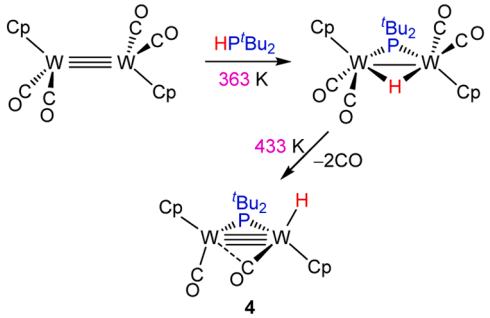

Scheme 2. Reaction of $[W_2Cp_2(CO)_4]$ with HP^tBu_2.

The IR spectrum of **4** (Table 1) displays two relatively low-frequency C−O stretches at 1796 (s) and 1731 (vs) cm^{-1} indicative of the presence of semibridging carbonyls, as found in the structurally characterized dimolybdenum analogue $[Mo_2Cp_2H(\mu\text{-}P^tBu_2)(CO)_2]$ (Mo−Mo = 2.5145 (3) Å; ν(CO) = 1813 (s), 1778 (vs) cm^{-1} in THF solution). The hydride ligand gives rise to a poorly shielded resonance at −0.06 ppm (J_{HP} = 31, J_{HW} = 37 Hz) indicative of its terminal coordination (cf. δ −0.71 ppm, J_{HP} = 31, J_{HW} = 99 for the related terminal isomer in the PCy_2-bridged complex $[W_2Cp_2H(\mu\text{-}PCy_2)(CO)_2]$) [9]. Moreover, the appearance of a single Cp resonance in both the ^1H and ^{13}C NMR spectra, as well as a single carbonyl resonance at 259.1 ppm in the latter spectrum, indicates that **4** undergoes in solution the same fluxional process than its Mo analogue [10], not further investigated here. Such a process implies the exchange of both W and CO environments, hence the averaging of chemical shifts of CO and Cp ligands, as well as H−W and P−W couplings, which take the values of 37 and 307 Hz. As expected, the latter figures compare well with the half-sum of values measured at low temperature for the terminal isomer of the mentioned hydride complex $[W_2Cp_2H(\mu\text{-}PCy_2)(CO)_2]$ (J_{HW} = 99, 0; J_{PW} = 379, 240 Hz) [9].

2.2. Preparation of the iodide-bridged precursor $[W_2Cp_2(\mu\text{-}I)(\mu\text{-}P^tBu_2)(CO)_2]$ (1b)

In order to prepare a ditungsten complex analogous to compound **3b** we have followed procedures previously developed for related PPh_2- and PCy_2-bridged complexes [2,9], which in our case starts with the reaction of the known unsaturated cationic complex $[W_2Cp_2(\mu\text{-}P^tBu_2)(CO)_4]BF_4$ [5a] with NaI in refluxing 1,2-dichloroethane solution to give the new iodide-bridged dicarbonyl complex $[W_2Cp_2(\mu\text{-}I)(\mu\text{-}P^tBu_2)(CO)_2]$ (**1b**) in high yield (Scheme 3).

Spectroscopic data for compound **1b** in solution (Table 1 and Experimental section) are comparable to those of its Mo_2 analogue **1a** except for the changes expected from the replacement of Mo with W (decrease in C − O stretches and ^{31}P chemical shift). We also note that the P−W coupling of 307 Hz in **1b** is slightly lower than the value of 317 Hz measured for the related PPh_2-bridged complex $[W_2Cp_2(\mu\text{-}I)(\mu\text{-}PPh_2)(CO)_2]$ [2], as expected from the lower electronegativity of the ^{t}Bu substituents (relative to Ph) at the P atom [13].

Table 1
Selected IR and $^{31}P\{^1H\}$ NMR data for new compounds.[a]

Compound	ν(XO)	δ (P)
$[Mo_2Cp_2(\mu\text{-}Cl)(\mu\text{-}P^tBu_2)(CO)_2]$ (**1a**)[b]	1889 (m), 1849 (vs)	215.9
$[W_2Cp_2(\mu\text{-}I)(\mu\text{-}P^tBu_2)(CO)_2]$ (**1b**)	1867 (m, sh), 1823 (vs)	148.5 [307]
syn,trans-$[Mo_2Cp_2Cl(\mu\text{-}P^tBu_2)(CO)(NO)_2]$ (**2a**)	1956 (vs), 1679 (s), 1623 (m)[c]	286.4
syn,trans-$[W_2Cp_2I(\mu\text{-}P^tBu_2)(CO)(NO)_2]$ (**2b**)	1963 (vs), 1662 (s), 1602 (m)	208.0 [274, 186]
$[Mo_2Cp_2(\mu\text{-}Cl)(\mu\text{-}P^tBu_2)(NO)_2]$ (**3a**)[d]	1602 (w, sh), 1575 (vs)	282.0
cis-$[Mo_2Cp_2(\mu\text{-}Cl)(\mu\text{-}P^tBu_2)(NO)_2]$ (***cis*-3a**)	1612 (vs), 1575 (m)	287.2
$[W_2Cp_2(\mu\text{-}I)(\mu\text{-}P^tBu_2)(NO)_2]$ (**3b**)	1576 (w, sh), 1555 (vs)	210.1 [334]
$[W_2Cp_2H(\mu\text{-}P^tBu_2)(CO)_2]$ (**4**)	1796 (s), 1731 (vs)	222.2 [307]
anti,cis-$[W_2Cp_2I(\mu\text{-}P^tBu_2)(CO)(NO)_2]$ (**5**)	1998 (vs), 1631 (s), 1592 (s)	200.8 [270, 127]
$[W_2Cp(\mu\text{-}\kappa\text{:}\eta^5\text{-}C_5H_4)I(\mu\text{-}P^tBu_2)(NH)(NO)]$ (**6**)	1575 (vs)[e]	186.5 [276, 217]

[a] IR spectra recorded in dichloromethane solution, unless otherwise stated, with stretching frequencies of NO and CO ligands (ν(XO), X = C, N) given in wave numbers (cm^{-1}); NMR spectra recorded in CD_2Cl_2 solution at 121.48 MHz and 293 K, unless otherwise stated, with chemical shifts (δ) in ppm relative to external 85 % aqueous H_3PO_4, and ^{31}P-^{183}W couplings (J) in hertz indicated between square brackets.

[b] Data taken from reference 10; IR data in THF solution; NMR data in C_6D_6 solution.

[c] In THF solution.

[d] Data taken from reference 1.

[e] ν(NO) = 1535 cm^{-1} in Nujol mull, see text.

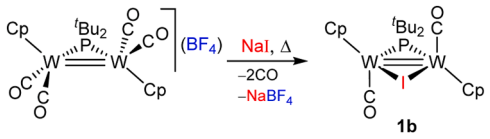

Scheme 3. Formation of compound **1b**.

2.3. Low-temperature reaction of compounds *1a,b* with NO

Compounds **1a,b** react readily with NO (5 % in N_2, 1 atm) at low temperature, whereby two NO molecules incorporate to the dimetal centre and one carbonyl ligand is displaced from it, to give a major product of composition $[M_2Cp_2X(\mu\text{-}P^tBu_2)(CO)(NO)_2]$ in each case. This first decarbonylation is faster for the Mo complex **1a** as expected, and it is completed actually at 233 K in ca. 45 min, to be compared to 273 K for the ditungsten complex in similar reaction times. Out of the eight possible isomers for such complexes, our data indicate that the major product corresponds in both cases to the isomer *syn,trans*-$[M_2Cp_2X(\mu\text{-}P^tBu_2)(CO)(NO)_2]$ (M = Mo, X = Cl (**2a**); M = W, X = I (**2b**)), with a *syn* arrangement of Cp ligands relative to the M_2P plane, and a transoid arrangement of the halide ligand X relative to the P atom. We note that the carbonyl ligand in both cases is placed in a cisoid arrangement relative to P (Scheme 4). The tungsten complex **2b** could be isolated as a crystalline material in a conventional way. However, the molybdenum complex **2a** undergoes progressive decarbonylation upon workup, and could not be isolated as a pure material.

The tungsten complex **2b** in the crystal (Fig. 1 and Table 2) displays two independent molecules in the unit cell, similar to each other. These are built from WCp(NO)(CO) and WCp(NO)I fragments bridged by a P^tBu_2 bridge in a slightly asymmetric way, with the P1–W2 length being some 0.02 Å shorter than the P1–W1 one, to balance the different electron counts (15 and 16e) of the corresponding metal fragments. In all, the molecule is an electron-precise, 34e complex, for which a single metal-metal bond has to be proposed, according to the 18e formalism, in agreement with the intermetallic separation of 3.113(1) Å (cf. 3.222(1) Å in $[W_2Cp_2(CO)_6]$ [14], or 3.194(1) Å in $[W_2Cp(\mu\text{-}PPh_2)(CO)_7]$) [15]. The local environments around the metal atoms in **2b** are of a distorted four-legged piano stool type, if we take into account the intermetallic interaction, with the Cp ligands positioned at the same side of the W_2P plane (*syn* conformation). The iodide ligand is placed in a transoid position relative to the P atom (P–W2–I = 130.9(1)°), whereas the carbonyl ligand is placed in a cisoid position relative to the same atom (P–W1–C1 = 84.2(6)°). Yet, the nitrosyl ligands define P–W–N angles close to 90° in both fragments (92.6(5) and 95.0(5)°, respectively).

Spectroscopic data in solution for compounds **2a** and **2b** (Table 1 and Experimental section) are similar to each other except for the changes expected from the replacement of Mo with W atoms, and consistent with the solid-state structure of **2b**. In particular, we note that the IR spectrum of these complexes display, in addition to a very strong C–O stretch at ca. 1960 cm^{-1}, two N–O stretches with relative intensities (strong and medium, in order of decreasing frequencies) characteristic of cisoid $[M(NO)]_2$ oscillators [16,17]. This is fully consistent with the acute N–W–W–N torsion angle of ca. 25° defined by the nitrosyl ligands of **2b** in the crystal, which in turn is related with the *syn* arrangement of the Cp ligands relative to the W_2P plane of the molecule.

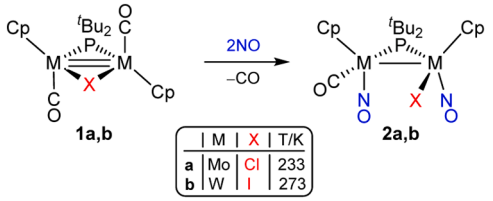

Scheme 4. Low-temperature reaction of compounds **1a,b** with NO.

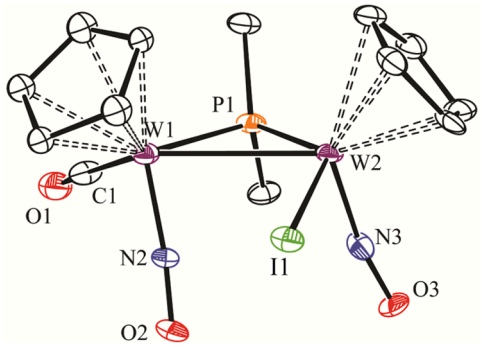

Fig. 1. ORTEP diagram (30 % probability) of one of the two independent molecules of compound **2b**, with ^{t}Bu groups (except their C^1 atoms) and H atoms omitted for clarity.

Table 2
Selected bond lengths (Å) and angles (°) for compound **2b**.

W1–W2	3.113(1)	W1–P1–W2	77.8(2)
W1–P1	2.489(5)	P1–W1–C1	84.2(6)
W2–P1	2.467(5)	P1–W1–N2	95.0(5)
W1–C1	1.99(2)	P1–W2–I1	130.9(1)
W1–N2	1.79(1)	P1–W2–N3	92.6(5)
W2–I1	2.833(2)	C1–W1–N2	87.7(7)
W2–N3	1.79(2)	I1–W2–N3	88.4(5)

We notice that the ^{31}P NMR resonance of **2b** displays two very different $^{31}P-^{183}W$ couplings of 274 and 186 Hz, in agreement with the distinct coordination spheres of the metal centres in these molecules, even if their coordination numbers are identical [13]. We finally note that the ^{t}Bu groups in these complexes givete rise to very broad resonances in the corresponding ^{1}H and ^{13}C NMR spectra (see the SI) when recorded at room temperature, which suggests slow rotation of the corresponding methyl groups, likely due to severe steric crowding. Indeed, in the case of **2b**, on lowering of the temperature these resonances progressively split and sharpen to render six distinct methyl resonances, as expected for the static structure of such an asymmetric molecule.

2.4. Decarbonylation reactions of the tungsten complex *2b*

Thermal decarbonylation reactions of **2b** were quite sensitive to experimental conditions, particularly solvent and temperature. The targeted dinitrosyl complex $[W_2Cp_2(\mu\text{-}I)(\mu\text{-}P^tBu_2)(NO)_2]$ (**3b**) was most efficiently prepared (in ca. 40 % yield after workup) in boiling propylbenzene solution (ca. 443 K) (Scheme 5). Under these conditions, the carbonyl complex *anti,cis*-$[W_2Cp_2I(\mu\text{-}P^tBu_2)(CO)(NO)_2]$ (**5**), an isomer of **2b**, was also isolated from the reaction mixture in ca. 5 % yield. Additionally, two cyclopentadienylidene-bridged products were unexpectedly formed in very small and variable amounts (<5 % relative to the

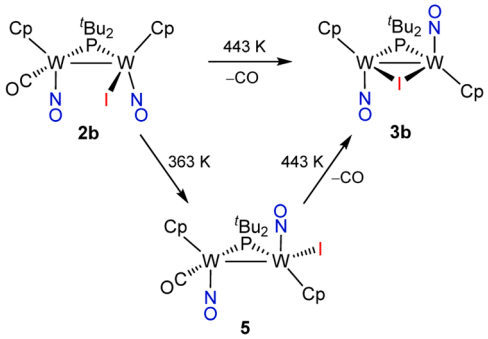

Scheme 5. Decarbonylation reactions of **2b**.

major product **3b**), with unknown origin: the previously reported dinitrosyl complex [$W_2Cp(\mu$-κ:η^5-$C_5H_4)(\mu$-$P^tBu_2)(CO)(NO)_2$] [5a], and the new imide nitrosyl complex [$W_2Cp(\mu$-κ:η^5-$C_5H_4)I(\mu$-$P^tBu_2)(NH)(NO)$] (**6**) (Chart 1). Compound **5** is an isomer of the starting compound **2b** more resistant to decarbonylation than it; yet, heating propylbenzene solutions of **5** at 443 K slowly induced its decarbonylation to yield **3b** in good yield. In addition, independent experiments revealed that compound **5** could be formed selectively from **2b** upon gentle heating of toluene solutions of the latter compound at 363 K (Scheme 5). As for the imide complex **6**, we note that its formation requires a rather complex sequence of unusual events: (a) C−H bond cleavage of a cyclopentadienyl ligand, presumably to yield cyclopentadienylidene (C_5H_4), and hydride ligands [18]; (b) N−O bond cleavage of a nitrosyl ligand, with O atom-transfer to an (undetermined) external molecule, to presumably yield a nitride ligand [5,19,20]; and (c) hydride migration to the latter ligand, to yield the imido (nitrene) group eventually found at **6**. Unfortunately, we have not found the experimental conditions that would favour the formation of this unexpected product.

Spectroscopic data for **3b** (Table 1 and Experimental section) are comparable to those of its molybdenum analogue **3a** [1], except for the changes anticipated when replacing Mo with W atoms, already noted, and therefore deserve no detailed comments. We just note that the transoid arrangement of Cp and NO pairs of ligands is denoted in the IR spectrum by the appearance of two N−O stretches with relative intensities (weak and strong, in order of decreasing frequency) characteristic of transoid $[M(NO)]_2$ oscillators [16,17]. There is also a significant increase in the ^{31}P-^{183}W coupling of **3b** (334 Hz), when compared to the values measured for **2b** (274 and 186 Hz), which is consistent with the reduction in the coordination number of the W atoms operated upon decarbonylation [13].

The structure of **5** can be derived from that of precursor **2b** by rotation of the WI(NO) fragment, this actually yielding a molecule ca. 7.8 kcal/mol more stable, according to density functional theory (DFT) calculations discussed below (see Section 2.6). Spectroscopically, this is accompanied by a significant increase in the C−O stretching frequency (1998 vs. 1963 cm^{-1}, Table 1), and by a subtle change in the intensities of the N−O stretches, with the asymmetric stretch now being a bit stronger than the symmetric one (Figure S27). The latter is indicative of the presence of a transoid $[M(NO)]_2$ oscillator, in agreement with the N−W−W−N torsion angle of ca. 154° found in the DFT-optimized structure of the complex (see the Supplementary materials). We finally note that the IR spectrum of **5** is comparable to those of the structurally characterized dimolybdenum alkyl complexes [$Mo_2Cp_2R(\mu$-$PCy_2)(CO)(NO)_2$] (R = Me, CH_2Ph), these also displaying *anti* (Cp) and *trans* (NO) pairs of ligands, while the alkyl and carbonyl ligands are positioned *cis* to the bridging P atom [21].

The molecular structure of **6** in the crystal (Fig. 2 and Table 3) is built from two tungsten atoms bridged by a P^tBu_2 ligand, and by a cyclopentadienylidene ligand σ-bound to one metal atom (W2) and η^5-bound to the other one (W1). The latter atom completes its coordination sphere with terminal iodide and imide ligands, while W2 bears cyclopentadienyl and nitrosyl ligands, with the latter occupying a transoid position relative to the imide ligand. In all, this is a 34e complex for which a single-metal-metal bond has to be proposed, in agreement with the short intermetallic length of 2.9376(2) Å. The latter distance is significantly shorter than the one in **2a** (3.113(1) Å), a difference that

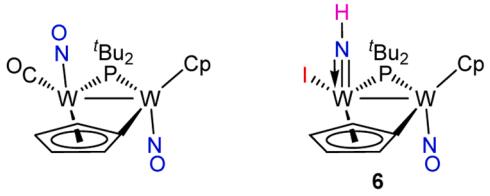

Chart 1. Trace side-products identified in decarbonylation reactions of **2b**.

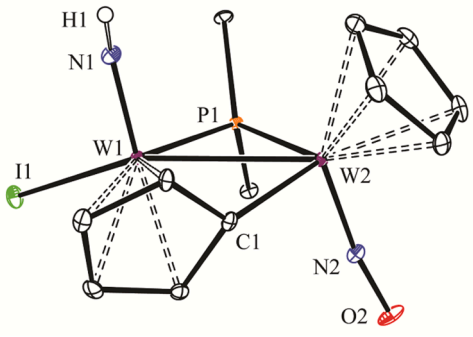

Fig. 2. ORTEP diagram (30 % probability) of compound **6**, with ^{t}Bu groups (except their C^1 atoms) and most H atoms omitted for clarity.

Table 3
Selected bond lengths (Å) and angles (°) for compound **6**.

W1−W2	2.9376(2)	W1−P1−W2	72.74(2)
W1−P1	2.4804(8)	P1−W1−I1	95.15(2)
W2−P1	2.4736(9)	P1−W1−N1	97.7(1)
W1−C1	2.199(3)	P1−W1−C1	7.0(1)
W1−N1	1.742(3)	P1−W2−C1	99.8(1)
W1−I1	2.7623(3)	P1−W2−N2	94.6(1)
W2−C1	2.102(3)	I1−W1−N1	102.9(1)
W2−N2	1.771(3)	C1−W2−N2	92.9(1)
N1−H1	0.85(5)	W1−N1−H1	151(4)

can be attributed to the presence here of a second bridging ligand with a bridgehead atom (C) of small covalent radius. The coordination of the cyclopentadienylidene ligand is comparable to that previously determined for the tungsten complex [$W_2Cp(\mu$-κ:η^5-$C_5H_4)(CO)_2(CN^tBu)(\mu$-$Ph_2PCH_2PPh_2)$] [22], or for the molybdenum dinitrosyl [$Mo_2Cp(\mu$-κ:η^5-$C_5H_4)(\mu$-$P^tBu_2)(CO)(NO)_2$] [23]. This involves a short σ-bond of 2.102(3) Å with the W2 atom, to be compared with M−C separations of 2.18(3) and 2.109(4) Å in the mentioned complexes, respectively.

As for the imide ligand, we note that the W−N distance is very short (1.742(3) Å), just a little longer than the average value of ca. 1.68 Å found for previously characterized nitride tungsten complexes [24], and comparable to the values of 1.73±0.01 Å measured for the three other NH tungsten complexes characterized previously by X-ray diffraction [25]. This length justifies the description of the NH ligand in **6** as a four-electron donor (neutral counting) involved in a W−N triple bond. Description of the latter would require using *sp* hybrids at the N atom, therefore a linear W−N−H arrangement; however, the actual W−N−H angle measured in **6** is 151(4)°. This bending can be attributed to the fact that the N-bound hydrogen is involved in substantial H-bonding with the O atom of the nitrosyl ligand of a nearby molecule (NH···O = 2.11(6) Å [26]), so as to configure an infinite chain of H-bonded molecules (Fig. 3). Spectroscopic evidence for this interaction is also found in the solid-state (Nujol mull) IR spectrum of **6**, which displays a N−H stretch at the relatively low frequency of 3202 cm^{-1} (cf. 3366 cm^{-1} in the amidinate complex [$Mo_2Cp_2(\mu$-$P^tBu_2)(\mu$-κN:$\kappa N'$-HNCMeNH)(μ-NO)]PF_6 [1], or ca. 3350 cm^{-1} in *trans*-[$Mo_2Cp_2(\mu$-$PCy_2)(\mu$-$NH_2)(NO)_2$]) [27]. This is accompanied by a decrease in the N−O stretch of the nitrosyl ligand, which appears at 1535 cm^{-1}, some 40 cm^{-1} below the observed frequency in dichloromethane solution (Table 1), since the nitrosyl ligand acquires an incipient hydroxyimide (N−OH) character as a result of the H-bonding interaction.

Spectroscopic data in solution for **6** are consistent with the structure in the crystal discussed above. Particularly informative is its ^1H NMR spectrum, which displays four distinct resonances for the inequivalent CH atoms of the cyclopentadienylidene ligand, and a quite deshielded resonance for the NH atom, which appears at 9.75 ppm as a broad 1:1:1 triplet due to coupling to the quadrupolar ^{14}N nucleus. The ^1H-^{14}N

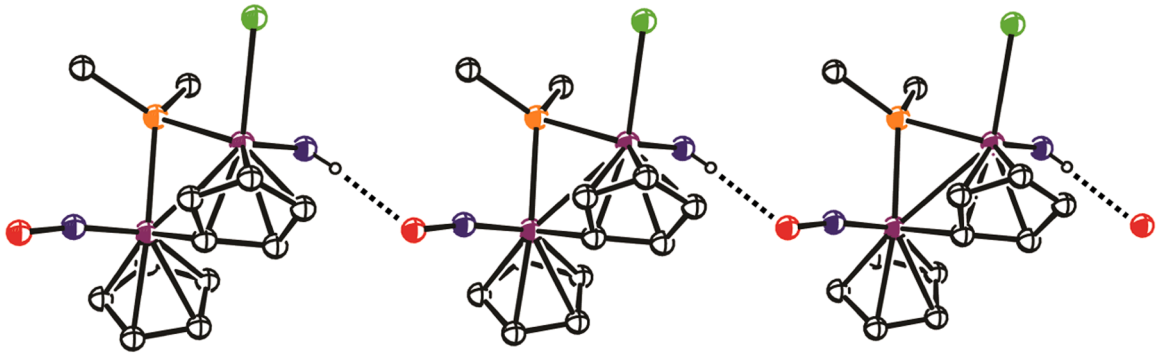

Fig. 3. Mercury-generated view of the H-bonded chain of molecules of **6** in the crystal lattice, with ^{t}Bu groups (except their C^{1} atoms) and most H atoms omitted for clarity (NH···O = 2.11(6) Å; N·····O = 2.866(5) Å; N−H···O = 148(4)°).

coupling of 49 Hz is close to the values of 50–55 Hz expected for metal imide complexes, based on data of ^{15}N-^{1}H couplings [28], but direct comparison with $J(^{1}H\text{-}^{14}N)$ values in complexes related to **6** is difficult since the corresponding NH atoms usually give rise to just broad resonances precluding the observation of any coupling.

2.5. Decarbonylation reactions of the molybdenum complex *2a*

Decarbonylation of the molybdenum complex **2a** proceeded more easily than that of its ditungsten analogue **2b**, as expected. In fact, it proceeds slowly at room temperature, although it is more conveniently completed by just refluxing toluene solutions of the complex for a few minutes. Under the latter conditions, the targeted complex [$Mo_2Cp_2(\mu$-Cl)(μ-P^{t}Bu$_2$)(NO)$_2$] (**3a**) is the major product formed, which could be isolated in 63 % yield (Scheme 6), as reported in our preliminary work on this chemistry [1]. However, more careful chromatographic workup of the reaction mixture enabled the isolation of two more new products: the *cis*-dinitrosyl isomer of the above complex, *cis*-[$Mo_2Cp_2(\mu$-Cl)(μ-P^{t}Bu$_2$)(NO)$_2$] (***cis*-3a**), isolated in 9 % yield, and tiny amounts (ca. 2 %) of a blue compound, not further investigated, which we could identify as the new trinitrosyl complex *trans*-[$Mo_2Cp_2(\mu$-P^{t}Bu$_2$)(μ-NO)(NO)$_2$] on the basis of spectroscopic similarities with its PCy$_2$-bridged analogue [5b,29]. The origin of this minor side-product is currently unknown. On the other hand, we note that a separate experiment indicated that ***cis*-3a** does not transform into its more stable transoid isomer **3a** in refluxing toluene solution, a matter to be further discussed below.

The transoid arrangement of nitrosyl ligands in **3a** is indicated by the relative intensities of the N−O stretches in the IR spectrum, weak and strong in order of decreasing frequencies (Table 1) [16]. This is reversed in ***cis*-3a**, which displays N−O stretches at 1612 (vs) and 1575 (m) cm^{-1}, thus revealing the presence of a cisoid [M(NO)]$_2$ oscillator defining a N−M−M−N dihedral angle close to 0° in the molecule (5° in the DFT-computed structure of the complex, see the Supplementary

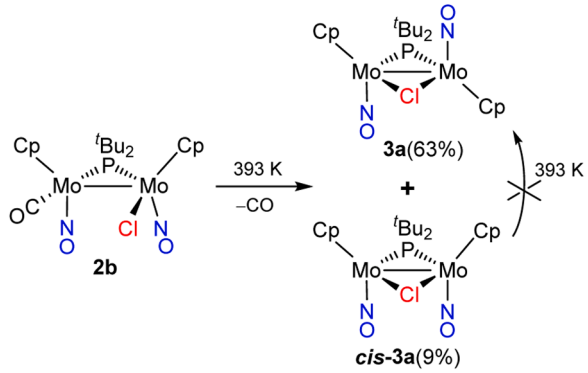

Scheme 6. Decarbonylation reaction of compound **2a**.

materials). On the other hand, the rotational C_2 axis present in **3a** relates the pairs of Cp and ^{t}Bu groups, which give rise to single ^{1}H and ^{13}C NMR resonances in each case (see the Experimental section). In contrast, a symmetry plane relates both metal fragments in isomer ***cis*-3a**, which renders equivalent Cp groups, but inequivalent ^{t}Bu groups. Indeed, the ^{1}H NMR spectrum of this isomer not only displays separate resonances for the ^{t}Bu groups of the molecule, but one of them is split at room temperature into two broad resonances at 1.83 and 0.34 ppm corresponding to 6 and 3 hydrogens, respectively. This indicates that rotation of the methyl groups in one of the ^{t}Bu substituents (likely the one close to both Cp ligands) is slow on the NMR timescale.

2.6. Reaction pathways in the thermal decarbonylation of compounds *2a, b*

In the preceding sections we have noted that decarbonylation of compounds **2a** and **2b**, while leading to the same type of major product (**3a** and **3b**), differ in the minor products. Most notably, an isomer of the main product is formed in the case of the molybdenum complex (***cis*-3a**), but an isomer of the starting compound in the case of the tungsten complex (**5**). By taking into account the experimental findings, already noted, revealing that complex ***cis*-3a** does not rearrange into **3a**, but that **2b** rearranges into **5** under mild conditions, while the latter undergoes decarbonylation slowly even at 443 K, we propose for the decarbonylation of compounds **2** the three reaction pathways shown in Scheme 7. In order to determine the thermodynamic profile for the different pathways proposed, the structures of the intermediates and products appearing in that Scheme have been computed using DFT methods (see the Experimental section and the Supplementary materials), and their relative Gibbs free energies are collected in Fig. 4. First of all, we note that the coordination position of the halide ligand in compounds **2**, *trans* to the P atom, is ideally suited for moving into a bridging position after decarbonylation of the molecule. This naturally renders the *cis* isomers of compounds **3**, but this seems to be a competitive reaction pathway only for the molybdenum complex, in agreement with the higher thermodynamic gap to overcome in the tungsten case (ΔG_r = 15.9 kcal/mol for **2b**→***cis*-3b**+CO, a gap much higher than the ones for other alternatives).

The experimentally observed isomerization **2b**→**5** (**5b** in calculations) requires rotation of the WCpI(NO) fragment to drive the halide ligand *cis* to the P atom (isomerization 1 in Scheme 7). This is computed to be an exergonic process for both the tungsten system (7.8 kcal/mol below **2b**) and for the molybdenum one (4.2 kcal/mol below **2a**). Decarbonylation from isomers **5** is more difficult than that from the parent isomers **2**, particularly for the tungsten system (ΔG_r = 17.6 kcal/mol for **5b**→**3b**+CO), and the kinetic barrier is expected to be considerably high, as the halide ligand is not positioned in the right position to move into the bridging mode, all of which is in agreement with the slow decarbonylation of **5** even at 443 K, a circumstance enabling its

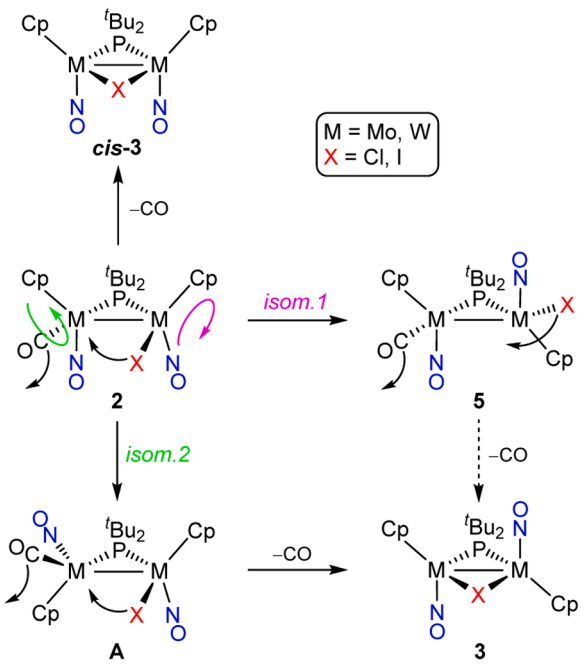

Scheme 7. Reaction pathways to compounds **3a,b**.

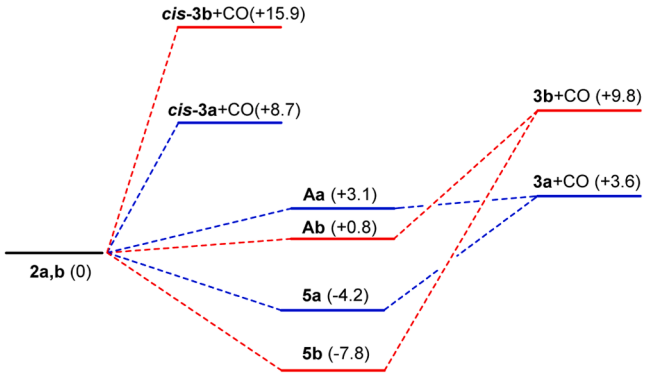

Fig. 4. M06L-DFT computed thermodynamic profile for the reactions shown in Scheme 7 for either molybdenum (**a**, blue) or tungsten (**b**, red) complexes, with standard Gibbs free energies in kcal/mol, relative to the corresponding parent compound of type **2**, shown between parenthesis.

detection and isolation. In fact, the most straightforward path connecting compounds **2** and **3** would start with the alternative rotation of the WCp(CO)(NO) fragment (isomerization 2 in Scheme 7), since this leaves the Cp ligands in the same *anti* arrangement found in the final product **3**, while keeping the halide ligand ready to rearrange into a bridging position. Such an isomerization would yield intermediates **A**, computed to be only slightly less stable than the parent substrates **2**, by 3.1 (Mo) or just 0.8 kcal/mol (W). These intermediates would then decarbonylate easily to give the final products **3** with a very reduced thermodynamic gap of 0.5 kcal/mol for the molybdenum complex, and with a moderate one (9 kcal/mol) for the tungsten complex. It is possible that this third pathway is operative in the very slow decarbonylation of compound **5** to give **3b** (through the sequence **5→2b→Ab→3b**), although an alternative, more direct path, cannot be excluded.

3. Conclusions

The halide nitrosyl complexes of type $[M_2Cp_2X(\mu\text{-}P^tBu_2)(CO)(NO)_2]$ (M = Mo, X = Cl; M = *W, X = I*) can be easily prepared through the low-temperature reaction of the corresponding unsaturated dicarbonyls $[M_2Cp_2(\mu\text{-}X)(\mu\text{-}P^tBu_2)(CO)_2]$ with NO. Out of the eight possible isomers, these products are specifically obtained with a *syn* arrangement of Cp ligands relative to the M_2P plane, and a *trans* positioning of the halide relative to phosphorus (*syn,trans*-isomers), while the carbonyl ligand is positioned *cis* with respect to the same P atom. These are kinetic isomers which at higher temperatures evolve through at least three different reaction pathways. The dominant pathway in both cases seems to involve first a slightly endergonic rearrangement of the MCp(CO)(NO) fragment to reach an *anti* positioning of the Cp ligands, followed by decarbonylation and halide movement into the bridging position, to give the major products *trans*-$[M_2Cp_2(\mu\text{-}X)(\mu\text{-}P^tBu_2)(NO)_2]$. Alternatively, direct decarbonylation would be also possible for the above *syn,trans* isomers, with halide rearrangement into the bridging position, to give a cisoid isomer of the major product, *cis*-$[M_2Cp_2(\mu\text{-}X)(\mu\text{-}P^tBu_2)(NO)_2]$, but this is only observed for the molybdenum complex, for which direct decarbonylation is thermodynamically more accessible (by some 7 kcal/mol, according to DFT calculations). The third reaction path involves a moderately exergonic rearrangement of the MCpX(NO) fragment to reach an *anti* positioning of the Cp ligands, thus rendering *anti,cis* isomers of the parent compound. Because of the cisoid positioning of the halide ligand relative to the P atom in these isomers, their evolution into halide-bridged products is expected to be difficult after decarbonylation, particularly for the tungsten system, with a large thermodynamic gap of some 18 kcal/mol to be overcome under standard conditions. All of this is consistent with our ability to isolate such a ditungsten isomer (*anti,cis*-$[W_2Cp_2I(\mu\text{-}P^tBu_2)(CO)(NO)_2]$), and to even make it a major product when heating the parent *syn,trans* isomer at moderate temperature.

4. Experimental

4.1. General procedures and starting materials

All manipulations and reactions were carried out under an argon (99.995 %) atmosphere using standard Schlenk techniques. Solvents were purified according to literature procedures, and distilled prior to use [30]. Compounds $[W_2Cp_2(CO)_6]$ [31], $[Mo_2Cp_2(\mu\text{-Cl})(\mu\text{-}P^tBu_2)(CO)_2]$ (**1a**) [10], and $[W_2Cp_2(\mu\text{-}P^tBu_2)(CO)_4](BF_4)$ [5a], were prepared as described previously. All other reagents were obtained from commercial suppliers and used as received, unless otherwise stated. Petroleum ether refers to that fraction distilling in the range 338–343 K. Filtrations were carried out through diatomaceous earth unless otherwise stated. Chromatographic separations were performed using jacketed columns cooled by tap water (ca. 288 K) or by a closed 2-propanol circuit kept at the desired temperature with a cryostat. Commercial aluminium oxide (activity I, 70–290 mesh) was degassed under vacuum prior to use. The latter was mixed under argon with the appropriate amount of water to reach activity IV. Silica gel (230–400 mesh) was used as received. IR stretching frequencies of NO and CO ligands were measured in solution (using CaF_2 windows), are referred to as ν(XO) (X = N, C), and are given in wave numbers (cm^{-1}). Nuclear magnetic resonance (NMR) spectra were routinely recorded at 295 K unless otherwise stated. Chemical shifts (δ) are given in ppm, relative to internal tetramethylsilane (^1H, ^{13}C), or external 85 % aqueous H_3PO_4 solutions (^{31}P). Coupling constants (J) are given in hertz.

4.2. Improved preparation of $[W_2Cp_2(\mu\text{-}H)(\mu\text{-}P^tBu_2)(CO)_4]$

A propylbenzene solution (15 mL) of $[W_2Cp_2(CO)_6]$ (0.750 g, 1.126 mmol) was refluxed for 7 h with a gentle N_2 purge to give a red-brown solution of $[W_2Cp_2(CO)_4]$, which was filtered with a canula. Neat PH^tBu_2 (313 μL, 1.690 mmol) was then added, and the mixture was stirred at 363 K for 16 h to give a red-brown solution. The solvent was then removed under vacuum, the residue was extracted with dichloromethane/petroleum ether (1/3), and the extracts were chromatographed on silica gel at 288 K. Elution with dichloromethane/petroleum ether (1/3) gave a yellow greenish band containing small amounts of the

known complex [WCpH(CO)$_3$] and other uncharacterized compounds, which was discarded. This was followed by a major red fraction yielding, upon removal of solvents, compound [$W_2Cp_2(\mu$-H)(μ-P^{t}Bu$_2$)(CO)$_4$] as a red microcrystalline solid (0.600 g, 70 %). Spectroscopic data for this complex were identical to those reported previously by us [5a]. Elution with dichloromethane/petroleum ether (3/1) gave a green fraction yielding, upon removal of solvents, compound [$W_2Cp_2H(\mu$-P^{t}Bu$_2$)(CO)$_2$] (**4**) as a green solid (0.022 g, 3 %; see below).

4.3. Preparation of [$W_2Cp_2H(\mu$-P^{t}Bu$_2$)(CO)$_2$] (**4**)

Compound [$W_2Cp_2(\mu$-H)(μ-P^{t}Bu$_2$)(CO)$_4$] (0.050 g, 0.066 mmol) was refluxed in propylbenzene (8 mL) at 443 K for 2.5 h with a gentle argon purge, to give a brown-greenish solution having compound **4** as the only P-containing species. Workup as described above gave first a red-brown fraction containing some [$W_2Cp_2(CO)_4$], then a green fraction yielding, after removal of solvents, compound **4** as a green powder (0.012 g, 26 %). Anal. Calcd for $C_{20}H_{29}O_2PW_2$: C, 34.31; H, 4.18. Found: C, 34.49; H, 3.78. ^{1}H NMR (400.13 MHz, CD_2Cl_2): δ 5.44 (s, 10H, Cp), 1.31 (d, J_{HP} = 14, 18H, ^{t}Bu), −0.06 (d, J_{HP} = 31, J_{HW} = 37, 1H, W−H). ^{13}C{^{1}H} NMR (100.63 MHz, C_6D_6): δ 259.1 (s, br, WCO), 91.4 (s, Cp), 46.7 [d, J_{CP} = 16, C^1(^{t}Bu)], 33.7 [d, J_{CP} = 4, C^2(^{t}Bu)].

4.4. Preparation of [$W_2Cp_2(\mu$-I)(μ-P^{t}Bu$_2$)(CO)$_2$] (**1b**)

Solid NaI (0.300 g, 2.000 mmol) was added to a 1,2-dichloroethane solution (12 mL) of [$W_2Cp_2(\mu$-P^{t}Bu$_2$)(CO)$_4$](BF$_4$), as prepared in situ from [$W_2Cp_2(\mu$-H)(μ-P^{t}Bu$_2$)(CO)$_4$] (0.200 g, 0.265 mmol). The mixture was first stirred at room temperature for 30 min, and then refluxed for 2.5 h to give a black greenish solution that was filtered using a canula. Removal of the solvent from the filtrate under vacuum and washing of the residue with petroleum ether (3 × 5 mL) yielded compound **1b** as a black solid (0.190 g, 87 %). Anal. Calcd for $C_{20}H_{28}O_2IPW_2$: C, 29.08; H, 3.42. Found: C, 29.10; H, 3.61. ^{1}H NMR (400.13 MHz, CD_2Cl_2): δ 5.39 (s, 10H, Cp), 1.35 (d, J_{HP} = 14, 18H, ^{t}Bu). ^{13}C{^{1}H} NMR (100.63 MHz, C_6D_6): δ 238.2 (d, J_{CP} = 5, WCO), 87.6 (Cp), 47.9 [d, J_{CP} = 18, C^1(^{t}Bu)], 33.1 [d, J_{CP} = 4, C^2(^{t}Bu)].

4.5. Preparation of solutions of syn,trans-[$Mo_2Cp_2Cl(\mu$-P^{t}Bu$_2$)(CO)(NO)$_2$] (**2a**)

Nitric oxide (5 % in N_2) was gently bubbled at 233 K for 45 min through a tetrahydrofuran solution (15 mL) containing ca. 1 mmol [$Mo_2Cp_2(\mu$-Cl)(μ-P^{t}Bu$_2$)(CO)$_2$], as prepared from [$Mo_2Cp_2(CO)_6$] (0.500 g, 1.020 mmol), to give a dark orange solution containing compound **2a** as a major product, contaminated with small amounts of **3a** and other unidentified species (see the Supplementary material). No further purification of this product was possible, as it easily undergoes decarbonylation at room temperature or under vacuum. The NMR spectra of this intermediate complex were recorded by carrying out the above reaction in CD_2Cl_2 (1 mL), and starting from ca. 0.1 mmol of complex [$Mo_2Cp_2(\mu$-Cl)(μ-P^{t}Bu$_2$)(CO)$_2$]. ^{1}H NMR (300.13 MHz, CD_2Cl_2): δ 5.86 (d, J_{HP} = 1, 5H, Cp) 5.55 (s, 5H, Cp), 1.40 (vbr, 9H, ^{t}Bu), 1.23 (d, J_{HP} = 15, 9H, ^{t}Bu).

4.6. Preparation of syn,trans-[$W_2Cp_2I(\mu$-P^{t}Bu$_2$)(CO)(NO)$_2$] (**2b**)

Nitric oxide (5 % in N_2) was gently bubbled through a tetrahydrofuran solution (12 mL) of compound **1b** (0.190 g, 0.230 mmol) at 273 K for 45 min, to give a dark red solution which was filtered. Removal of solvent from the filtrate under vacuum and washing of the residue with petroleum ether (2 × 5 mL) gave an orange solid containing essentially pure compound **2b** (0.160 g, 81 %) ready for further use. The crystals used for the X-ray diffraction study of this compound were grown by the slow diffusion of layers of toluene and petroleum ether into a concentrated dichloromethane solution of the crude complex at 253 K. Anal. Calcd for $C_{19}H_{28}O_3N_2IPW_2$: C, 26.60; H, 3.29; N, 3.26. Found: C, 26.19; H, 3.49; N, 2.98. ^{1}H NMR (400.13 MHz, CD_2Cl_2): δ 5.89, 5.71 (2 s, 2 × 5H, Cp), 1.47 (vbr, 18H, ^{t}Bu). ^{1}H NMR (400.13 MHz, CD_2Cl_2, 213 K): δ 5.88, 5.68 (2 s, 2 × 5H, Cp), 1.80 (d, J_{HP} = 11, 3H, ^{t}Bu), 1.78 (d, J_{HP} = 10, 3H, ^{t}Bu), 1.45 (d, J_{HP} = 13, 3H, ^{t}Bu), 1.34 (d, J_{HP} = 15, 3H, ^{t}Bu), 0.87 (d, J_{HP} = 18, 3H, ^{t}Bu), 0.68 (d, J_{HP} = 17, 3H, ^{t}Bu). ^{13}C{^{1}H} NMR (100.63 MHz, CD_2Cl_2): δ 221.5 (d, J_{CP} = 14, WCO), 97.6, 94.0 (2 s, Cp), 50.4 [d, J_{CP} = 16, C^1(^{t}Bu)], 44.6 [d, J_{CP} = 12, C^1(^{t}Bu)], 33.7 [s, br C^2(^{t}Bu)], 32.6 [s, C^2(^{t}Bu)]. ^{13}C{^{1}H} NMR (100.63 MHz, CD_2Cl_2, 213 K): δ 220.8 (d, J_{CP} = 14, WCO), 96.9, 93.4 (2 s, Cp), 49.6 [d, J_{CP} = 16, C^1(^{t}Bu)], 43.8 [d, J_{CP} = 12, C^1(^{t}Bu)], 36.8 [s, C^2(^{t}Bu)], 33.5 [d, J_{CP} = 8, C^2(^{t}Bu)], 32.3 [d, J_{CP} = 7, C^2(^{t}Bu)], 31.4 [s, 2C^2(^{t}Bu)], 29.7 [s, C^2(^{t}Bu)].

4.7. Decarbonylation of compound **2a**

Nitric oxide (5 % in N_2) was gently bubbled at 233 K for 45 min through a tetrahydrofuran solution (15 mL) containing ca. 1 mmol of [$Mo_2Cp_2(\mu$-Cl)(μ-P^{t}Bu$_2$)(CO)$_2$], as prepared from [$Mo_2Cp_2(CO)_6$] (0.500 g, 1.020 mmol), to give a dark orange solution containing compound **2a** as a major product. After removal of the solvent under vacuum, the residue was dissolved in toluene and refluxed for 15 min to give a yellow-brown solution. The solvent was again removed, the residue was extracted with dichloromethane/petroleum ether (1/2), and the extracts were chromatographed on alumina at 288 K. Elution with the same solvent mixture gave a major yellow fraction yielding, after removal of solvents, compound **3a** as a yellow powder (0.360 g, 64 %). Elution with dichloromethane/petroleum ether (1/1) gave a very minor blue fraction yielding analogously the trinitrosyl complex [$Mo_2Cp_2(\mu$-P^{t}Bu$_2$)(μ-NO)(NO)$_2$] as a blue solid (0.010 g, 2 %), not further investigated (see Section 2.5). Finally, elution with dichloromethane/petroleum ether (3/1) gave a second yellow fraction yielding analogously compound ***cis*-3a** as a yellow solid (0.050 g, 9 %). Spectroscopic data for **3a** were as reported previously [1]. *Data for **cis-3a***: Anal. Calcd for $C_{18}H_{28}O_2ClMo_2N_2P$: C, 38.42; H, 5.02; N, 4.98. Found: C, 38.05; H, 5.27; N, 4.66. ^{1}H NMR (400.13 MHz, CD_2Cl_2): δ 5.75 (s, 10H, Cp), 1.83 (s, br, 6H, ^{t}Bu), 1.44 (d, J_{HP} = 15, 9H, ^{t}Bu), 0.34 (s, vbr, 3H, ^{t}Bu). ^{13}C{^{1}H} NMR (100.63 MHz, CD_2Cl_2): δ 97.4 (s, Cp), 49.3 [d, J_{CP} = 11, C^1(^{t}Bu)], 41.3 [d, J_{CP} = 7, C^1(^{t}Bu)], 35.6 [s, vbr, 1C^2(^{t}Bu)], 34.4 [d, J_{CP} = 5, 3C^2(^{t}Bu)], 34.0 [s, br, 2C^2(^{t}Bu)].

4.8. Decarbonylation of compound **2b**

A propylbenzene solution (15 mL) of crude compound **2b** (0.160 g, 0.186 mmol), prepared as described above, was heated at 363 K for 30 min, then refluxed for 4.5 h with a gentle argon purge to give an orange-brown solution. After removal of the solvent under vacuum, the residue was extracted with dichloromethane/petroleum ether (1/1), and the extracts were chromatographed on alumina at 288 K. Elution with the same solvent mixture gave a minor yellow fraction yielding, upon removal of solvents, compound *anti,cis*-[$W_2Cp_2I(\mu$-P^{t}Bu$_2$)(CO)(NO)$_2$] (**5**) as an orange solid (0.008 g, 5 %, see Section 4.9). Elution with dichloromethane/petroleum ether (2/1) gave a major fraction yielding analogously [$W_2Cp_2(\mu$-I)(μ-P^{t}Bu$_2$)(NO)$_2$] (**3b**) as an orange solid (0.060 g, 39 %), then a very minor purple fraction yielding compound [$W_2Cp(\mu$-κ:η^5-C$_5$H$_4$)I(μ-P^{t}Bu$_2$)(NH)(NO)] (**6**) as a purple solid (usually less than 0.003 g, 2 %). The crystals used in the X-ray diffraction study of the latter compound were grown by the slow diffusion of layers of toluene and petroleum ether into a concentrated dichloromethane solution of the complex at 253 K. *Data for compound **3b***: Anal. Calcd for $C_{18}H_{28}O_2N_2IPW_2$: C, 26.05; H, 3.40; N, 3.38. Found: C, 26.30; H, 3.71; N, 3.22. ^{1}H NMR (400.13 MHz, CD_2Cl_2): δ 5.79 (s, 10H, Cp), 1.37 (d, J_{HP} = 14, 18H, ^{t}Bu). ^{13}C{^{1}H} NMR (100.63 MHz, CD_2Cl_2): δ 93.6 (s, Cp), 47.0 [d, J_{CP} = 16, C^1(^{t}Bu)], 33.5 [d, J_{CP} = 4, C^2(^{t}Bu)]. *Data for compound **6***: Anal. Calcd for $C_{18}H_{28}ON_2IPW_2$: C, 26.56; H, 3.47; N, 3.44. Found: C, 26.35; H, 3.10; N, 2.94. IR (Nujol mull): 3202 (br, N−H), 1535 (vs, N−O) cm^{-1}. ^{1}H NMR (300.13 MHz, CD_2Cl_2): δ 9.75 (t, br, J_{14NH} = 49,

1H, NH), 6.48, 6.25, 5.23, 4.44 (4 m, 4 × 1H, C_5H_4), 5.82 (s, 5H, Cp), 1.52 (d, J_{HP} = 14, 9H, ^{t}Bu), 1.37 (s, br, 9H, ^{t}Bu).

4.9. Preparation of anti,cis-[$W_2Cp_2I(\mu$-P^{t}Bu$_2$)(CO)(NO)$_2$] (5)

A toluene solution (10 mL) of crude compound **2b**, prepared from [$W_2Cp_2(\mu$-H)(μ-P^{t}Bu$_2$)(CO)$_4$] (0.050 g, 0.066 mmol) as described above, was heated at 363 K for 30 min, to give an orange solution. After removal of the solvent under vacuum, the residue was extracted with dichloromethane/petroleum ether (1/2), and the extracts were chromatographed on alumina at 288 K. Elution with the same solvent mixture gave a minor red fraction containing a little [$W_2Cp_2(CO)_6$]. Elution with dichloromethane/petroleum ether (1/1) gave a major orange fraction yielding, upon removal of solvents, compound **5** as an orange solid (0.022 g, 55 %). Anal. Calcd for $C_{19}H_{28}O_3N_2IPW_2$: C, 26.60; H, 3.29; N, 3.26. Found: C, 26.90; H, 3.50; N, 3.31. ^{1}H NMR (400.13 MHz, CD_2Cl_2): δ 5.84, 5.80 (2 s, 2 × 5H, Cp), 1.42, 1.37 (2d, J_{HP} = 15, 2 × 9H, ^{t}Bu). ^{13}C{^{1}H} NMR (100.63 MHz, CD_2Cl_2): δ 217.2 (d, J_{CP} = 15, WCO), 100.8, 96.2 (2 s, Cp), 48.1 [d, J_{CP} = 13, C^1(^{t}Bu)], 46.1 [d, J_{CP} = 12, C^1(^{t}Bu)], 33.8 [d, J_{CP} = 4, C^2(^{t}Bu)], 33.7 [d, J_{CP} = 3, C^2(^{t}Bu)].

4.10. X-Ray structure determination of compounds 2b and 6

Data collection for these compounds was performed at ca. 100 K on a Bruker D8 Venture Photon III 14 κ-geometry diffractometer, using MoK$_\alpha$ radiation. The software APEX3 [32] was used for collecting frames with the ω/ϕ scan measurement method. The SAINT V8.40B software was used for data reduction [33], and a multi-scan absorption correction was applied with SADABS-2016/2 [34]. Using the program suite WinGX [35], the structures were solved by Patterson interpretation and phase expansion using SHELXL2018/3 [36], and refined with full-matrix least squares on F^2 using SHELXL2018/3. In general, all non-hydrogen atoms were refined anisotropically, except for atoms involved in disorder, and all hydrogen atoms were geometrically placed and refined using a riding model. In compound **2b**, two similar but independent molecules of the complex (and of dichloromethane) were present in the unit cell, each of them displaying a disordered cyclopentadienyl ligand, satisfactorily modelled over two sites with 0.50/0.50 occupancies. All non-hydrogen atoms were refined anisotropically, except for C(1) and the carbon atoms involved in the modelled disorders, which were refined isotropically to prevent their temperature factors from becoming non-positive definite, this causing the appearance of a B-level alert in the corresponding checkcif file. Because of the poor quality of the crystal, some splitting in many reflections was apparent, but this could not be treated as a twin. This is the most likely origin of the significant electron density residuals obtained after convergence in the vicinity of the tungsten atoms (up to 7.14 eÅ^{-3}), and of the poor agreement parameters eventually reached (R_1 = 8.05 %), therefore of a relatively low precision on the C−C distances, this causing a second B-level alert in the checkcif file. Yet, the geometry of the complex was well defined. In compound **6**, the N-bound hydrogen atom H(1) was located in the Fourier map and refined riding on its parent atom.

4.11. Computational details

All DFT calculations were carried out using the GAUSSIAN16 package [37], and the M06L functional [38]. A pruned numerical integration grid (99,590) was used for all the calculations via the keyword Int=Ultrafine together with the empirical dispersion correction from Grimme and co-workers via the keyword GD3 [39]. Effective core potentials and their associated double-ζ LANL2DZ basis set were used for Mo, I and W atoms [40]. The light elements (P, Cl, N, O, C and H) were described with the 6–31G* basis [41]. Geometry optimizations were performed under no symmetry restrictions, using initial coordinates derived from the X-ray data. Frequency analysis was performed for all the stationary points to ensure that a minimum structure with no imaginary frequencies was achieved in each case.

CRediT authorship contribution statement

M. Angeles Alvarez: Writing – review & editing, Software, Investigation. **M. Esther García:** Writing – review & editing, Methodology, Investigation, Conceptualization. **Daniel García-Vivó:** Writing – review & editing, Software, Methodology, Investigation, Conceptualization. **Ana M. Guerra:** Writing – review & editing, Methodology, Investigation, Conceptualization. **Miguel A. Ruiz:** Writing – review & editing, Writing – original draft, Supervision, Project administration, Methodology, Investigation, Funding acquisition, Conceptualization.

Declaration of competing interest

The authors declare that they have no known competing financial interests or personal relationships that could have appeared to influence the work reported in this paper.

Data availability

Data will be made available on request.

Acknowledgment

We thank the MICIU and AEI of Spain and FEDER for financial support (Project PGC2021-123964NB-I00), the SCBI of the Universidad de Málaga, Spain, for access to computing facilities, and the X-Ray unit of the Universidad de Santiago de Compostela, Spain, for acquisition of diffraction data.

Supplementary materials

Supplementary material associated with this article can be found, in the online version, at doi:10.1016/j.jorganchem.2024.123147.

References

[1] M.A. Alvarez, M.E. García, D. García-Vivó, A.M. Guerra, M.A. Ruiz, Inorg. Chem. 63 (2024) 3207.
[2] M.A. Alvarez, M.E. García, D. García-Vivó, M.A. Ruiz, A. Toyos, Dalton Trans. 45 (2016) 13300.
[3] (a) M.A. Alvarez, M.E. García, D. García-Vivó, M.A. Ruiz, A. Toyos, Dalton Trans 46 (2017) 15317;
(b) M.A. Alvarez, M.E. García, D. García-Vivó, M.A. Ruiz, A. Toyos, Inorg. Chem. 57 (2018) 228.
[4] (a) For some examples of C≡N bond cleavage of nitriles by metal complexes see: Y. Takahashi, A. Tahara, T. Takao Organometallics 39 (2020) 2888;
(b) T. Kawashima, T. Takao, H. Suzuki, Angew. Chem. Int. Ed. 45 (2006) 485;
(c) B.K. Bennett, S. Lovell, J.M. Mayer, J. Am. Chem. Soc. 123 (2001) 4336;
(d) Y. Tanabe, H. Seino, Y. Ishii, M. Hidai, J. Am. Chem. Soc. 122 (2000) 1690;
(e) J.H. Freudenberger, R.R. Schrock, Organometallics 5 (1986) 398;
(f) R.R. Schrock, M.L. Listemann, L.G. Sturgeoff, J. Am. Chem. Soc. 104 (1982) 4291.
[5] (a) M.A. Alvarez, M.E. García, D. García-Vivó, A.M. Guerra, M.A. Ruiz, Inorg. Chem. 61 (2022) 14929;
(b) M.A. Alvarez, M.E. García, D. García-Vivó, A. Ramos, M.A. Ruiz, A. Toyos, Inorg. Chem. 57 (2018) 15314.
[6] (a) For previous work of other groups on N−O bond cleavage of nitrosyl ligands at binuclear complexes, see: Z. Cai, W. Tao, C.E. Moore, S. Zhang, C.R. Wade Angew. Chem. Int. Ed. 60 (2021) 21221;
(b) Y. Arikawa, Y. Otsubo, H. Fujino, S. Horiuchi, E. Sakuda, K. Umakoshi, J. Am. Chem. Soc. 140 (2018) 842;
(c) Y. Arikawa, J. Hiura, C. Tsuchii, M. Kodama, N. Matsumoto, K. Umakoshi, Dalton Trans 47 (2018) 7399;
(d) T. Suzuki, H. Tanaka, Y. Shiota, P.K. Sajith, Y. Arikawa, K. Yoshizawa, Inorg. Chem. 54 (2015) 7181;
(e) Y. Arikawa, T. Asayama, M. Moriguchi, S. Agari, M. Onishi, J. Am. Chem. Soc. 129 (2007) 14160;
(f) P. Legzdins, M.A. Young, R.J. Batchelor, F.W.B. Einstein, J. Am. Chem. Soc. 117 (1995) 8798.
[7] M.E. García, V. Riera, M.A. Ruiz, M.T. Rueda, D. Sáez, Organometallics 21 (2002) 5515.

[8] M.E. García, S. Melón, A. Ramos, M.A. Ruiz, Dalton Trans. (2009) 8171.
[9] (a) M.A. Alvarez, M.E. García, D. García-Vivó, M.A. Ruiz, M.F. Vega, Organometallics 29 (2010) 512;
(b) M.A. Alvarez, M.E. García, D. García-Vivó, M.A. Ruiz, M.F. Vega, Dalton Trans 43 (2014) 16044.
[10] M.A. Alvarez, M. Casado-Ruano, M.E. García, D. García-Vivó, M.A. Ruiz, Inorg. Chem. 56 (2017) 11336.
[11] D. García-Vivó, A. Ramos, M.A. Ruiz, Coord. Chem. Rev. 257 (2013) 2143.
[12] R.A. Jones, S.T. Schwab, A.L. Stuart, B.R. Whittlesey, T.C. Wright, Polyhedron 4 (1985) 1689.
[13] C.J. Jameson, in Phosphorus-31 NMR Spectroscopy in Stereochemical Analysis, J. G. Verkade, L.D. Quin, Eds., VCH, Deerfield Beach, FL, 1987, Chapter 6.
[14] R.D. Adams, D.M. Collins, F.A. Cotton, Inorg. Chem. 13 (1974) 1086.
[15] S.G. Shyu, W.J. Wu, Y.S. Wen, S.M. Peng, G.H. Lee, J. Organomet. Chem. 489 (1995) 113.
[16] P.S. Braterman, Metal Carbonyl Spectra, Academic Press, London, U. K., 1975.
[17] C. de la Cruz, N. Sheppard, Spectrochim. Acta Part A 78 (2011) 7.
[18] M.A. Alvarez, C. Alvarez, M.E. García, V. Riera, M.A. Ruiz, C. Bois, Organometallics 16 (1997) 2581, and references therein.
[19] For some examples of N−O bond cleavage of nitrosyl ligands by binuclear complexes see: M.A. Alvarez, M.E. García, M.A. Ruiz, A. Toyos, Inorg. Chem. 52 (2013) 3942, and references therein.
[20] (a) For some examples of N−O bond cleavage of nitrosyl ligands by mononuclear complexes see, for instance A.S. Veige, LeG.M. Slaughter, E.B. Lobkovsky, P. T. Wolczansky, N. Matsunaga, S.A. Decker, T.R. Cundari, Inorg. Chem. 42 (2003) 6204;
(b) A.L. Odom, C.C. Cummins, J.D. Protasiewicz, J. Am. Chem. Soc. 117 (1995) 6613.
[21] M.A. Alvarez, M.E. García, M.E. Martínez, A. Ramos, M.A. Ruiz, Organometallics 28 (2009) 6293.
[22] M.A. Alvarez, M.E. García, V. Riera, L.R. Falvello, C. Bois, Organometallics 16 (1997) 354.
[23] M.A. Alvarez, M.E. García, A.M. Guerra, M.A. Ruiz, CSD Communication, 2022, CCDC 2168555, DOI: 10.5517/ccdc.csd.cc2bskd3.
[24] A search at the Cambridge Crystallographic Data Centre database (updated March 2024) on tungsten complexes bearing terminal nitride ligands yielded just 16 complexes, almost all of them with W−N distances in the very narrow range of 1.68 ± 0.01Å.
[25] (a) G. Guillemot, E. Solari, C. Floriani, C. Rizzoli, Organometallics 20 (2001) 607;
(b) H. Ishino, S. Tokunaga, H. Seino, Y. Ishii, M. Hidai, Inorg. Chem. 38 (1999) 2489;
(c) D. Watanabe, S. Gondo, H. Seino, Y. Mizobe, Organometallics 26 (2007) 4909.
[26] J.E. Huheey, E.A. Keiter, R.L. Keiter, The reference NH···O hydrogen bonding length is 2.00Å. See, for instance. Inorganic Chemistry: Principles of Structure and Reactivity, 4th ed., HarperCollins College Publishers, New York, USA, 1993, p. 301.
[27] M.A. Alvarez, M.E. García, D. García-Vivó, M.A. Ruiz, A. Toyos, Inorg. Chem. 54 (2015) 10536.
[28] A value of 49 Hz for a 1H-14N coupling corresponds to 69Hz for an equivalent 1H-15N coupling, a figure close to the usual values of ca. 75Hz found in imide complexes. See J. Mason, in Multinuclear RMN, J. Mason (Ed.), Plenum Press, London, UK, 1987, chapter 12, p. 358.
[29] This blue complex displays N−O stretches in dichloromethane solution at 1618 (w, sh), 1589 (vs) cm−1, and a 31P chemical shift of 256.4ppm, to be compared to values of ν(N−O) = 1625 (w, sh), 1587 (vs) cm−1 and δP = 219.4ppm for its PCy2-bridged analogue in the same solvent (see reference 5b).
[30] W.L.F. Armarego, C. Chai, Purification of Laboratory Chemicals, 7th ed., Butterworth-Heinemann, Oxford, U. K., 2012.
[31] A.R. Manning, P. Hacket, R. Birdwhistell, P. Soye, Inorg. Synth. 28 (1990) 148.
[32] APEX3 v2019.11-0, Bruker AXS Inc., Madison (WI), USA, 2019.
[33] SAINT v8.40B, Bruker AXS Inc., Madison (WI), USA, 2018.
[34] L. Krause, R. Herbst-Irmer, G.M. Sheldrick, D. Stalke, J. Appl. Cryst. 48 (2015) 3.
[35] L.J. Farrugia, J. Appl. Crystallogr. 32 (1999) 837.
[36] (a) G.M. Sheldrick, SHELXL2018, University of Gottingen, Germany, 2018;
(b) G.M. Sheldrick, Acta Crystallogr. Sect. C 71 (2015) 5;
(c) G.M. Sheldrick, Acta Crystallogr. Sect. A 64 (2008) 112.
[37] M.J. Frisch, G.W. Trucks, H.B. Schlegel, G.E. Scuseria, M.A. Robb, J.R. Cheeseman, G. Scalmani, V. Barone, G.A. Petersson, H. Nakatsuji, X. Li, M. Caricato, A.V. Marenich, J. Bloino, B.G. Janesko, R. Gomperts, B. Mennucci, H.P. Hratchian, J.V. Ortiz, A.F. Izmaylov, J.L. Sonnenberg, D. Williams-Young, F. Ding, F. Lipparini, F. Egidi, J. Goings, B. Peng, A. Petrone, T. Henderson, D. Ranasinghe, V.G. Zakrzewski, J. Gao, Rega, N.; G. Zheng, W. Liang, M. Hada, M. Ehara, K. Toyota, R. Fukuda, J. Hasegawa, M. Ishida, T. Nakajima, Y. Honda, O. Kitao, H. Nakai, T. Vreven, K. Throssell, J.A. Montgomery, Jr., J.E. Peralta, F. Ogliaro, M.J. Bearpark, J.J. Heyd, E.N. Brothers, K.N. Kudin, V.N. Staroverov, T.A. Keith, R. Kobayashi, J. Normand, K. Raghavachari, A.P. Rendell, J.C. Burant, S.S. Iyengar, J. Tomasi, M. Cossi, J.M. Millam, M. Klene, C. Adamo, R. Cammi, J.W. Ochterski, R.L. Martin, K. Morokuma, O. Farkas, J.B. Foresman, D.J. Fox, Gaussian 16, Revision A.03, Gaussian, Inc., Wallingford CT, USA, 2016.
[38] Y. Zhao, D.G. Truhlar, J. Chem. Phys. 125 (2006) 194101, 1.
[39] S. Grimme, J. Antony, S. Ehrlich, H. Krieg, J. Chem. Phys. 132 (2010) 154104.
[40] P.J. Hay, W.R. Wadt, J. Chem. Phys. 82 (1985) 299.
[41] (a) P.C. Hariharan, J.A. Pople, Theor. Chim. Acta 28 (1973) 213;
(b) G.A. Petersson, M.A. AlLaham, J. Chem. Phys. 94 (1991) 6081;
(c) G.A. Petersson, A. Bennett, T.G. Tensfeldt, M.A. Al-Laham, W.A. Shirley, J. A. Mantzaris, J. Chem. Phys. 89 (1988) 2193.